Mikrochim. Acta 128, 169–175 (1998)

Mikrochimica Acta

Trace Level Vanadium Determination Using Thermal Lens Spectrophotometry

Manuel Caetano*, Leonardo Padrino T., Hector Gutiérrez, Alberto J. Fernández, and **Jimmy Castillo**

Escuela de Química, Facultad de Ciencias, Universidad Central de Venezuela, P.O. Box 47102, Caracas 1020a, Venezuela

Abstract. Trace level vanadium determination is reported using a dual beam thermal lens spectrometer. The thermal lens was generated using an argon ion beam laser (pump beam) which was focused into a sample cuvette. The thermal lens signal (TLs) was monitored with a He-Ne laser beam and a photodiode detector. Multichannel averager software was developed for processing the transient TLs. The optimal set up, ensuring maximum sensitivity and linear calibration graphs was obtained using experimental design techniques. Under optimized conditions, the detection limits for aqueous and ethanol-water (2+3 v/v) and (4+1 v/v) vanadium complex solutions were, respectively, 0.0071 mg/l, 0.0065 and 0.0039 mg/l.

Key words: thermal lens, vanadium analysis, trace analysis, spectrophotometry, optimization.

The aim of this work was to set up and evaluate a thermal lens spectrophotometer for analytical application in the quantitative determination of trace amounts of vanadium. The industrial use of vanadium is widespread in the industry, catalyst industry, ceramic and electronic equipment. This element in trace amounts is an essential element for cell growth at $\mu g\ l^{-1}$ levels, but can be toxic at higher concentrations. The toxicity of vanadium is dependent on its oxidation state [1], vanadium (V) being more toxic than vanadium (IV).

Spectrophotometry is the most common technique used for vanadium determination, owing to the good sensitivity and selectivity achieved. With a correct choice of reagents it is also possible to distinguish between the various oxidation states of vanadium [2]. However, spectrophotometry is not sensitive enough for accurate detection of minute amounts of vanadium, which can still be toxic. In some case, the detection limit can be improved by using a large amount of the sample or by using tedious analytical procedures such as organic solvent extraction [2].

Thermooptical techniques, i.e., thermal lens [3] photothermal deflection [8] are recognized methods for the quantitative determination of several metal and non-metal complexes, especially useful for ultratrace level determination of samples which do not exhibit fluorescence. These techniques have been applied for on-line detection of different metal species [9] and is adequate to develop a compact optical fiber instrument for remote sensing in process stream monitoring and environment analysis [5].

In thermooptical techniques, a temperature rise is produced in a sample medium by nonradiative relaxation of the absorbed energy from a modulated optical source, such as a laser beam. Since the refractive index of most materials changes with temperature, this temperature rise generates a perturbation of the refractive index of sample, which acts as an optical element.

In thermal lens spectroscopy (TLS), the effect is probed as a relative change in the beam center intensity of a probe laser, passing through the center of the lens (thermal lens) induced by the excitation beam [10]. In a steady state thermal lens configuration the signal (TLs) could be defined as [11].

$$TLs = \frac{I_0 - I_\infty}{I_0} \qquad (1)$$

Where I_0 and I_∞ are the intensities of the probe laser at the beam's center when $t = 0$ and $t \gg t_c$ the

* To whom correspondence should be addressed

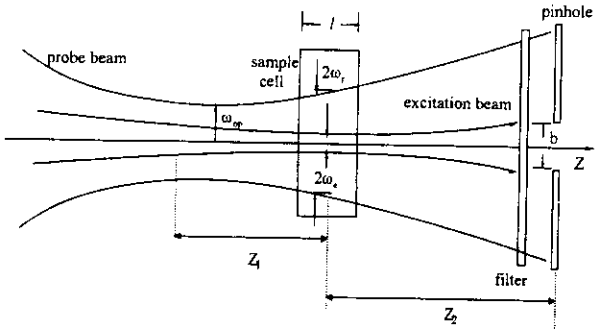

Fig. 1. Schematic representation of the dual-beam mode-mismatched thermal lens optical configuration. ω_p and ω_e are the radius of the probe and excitation beam at cell center; ω_{op} is the radius of the probe beam at its focus; Z_1 is the distance from the center of the sample to the waist of the probe beam; Z_2 is the distance from the center of the sample to the aperture; b is the aperture diameter and l is the sample cell length

characteristic constant time of the thermal lens, respectively.

Higher sensitivities have been obtained using a dual-beam mode-mismatched thermal lens optical configuration [7]. In Fig. 1 a schematic diagram of this configuration is shown, where a TEM_{00} Gaussian beam is focused in a cell containing an absorbing sample causing a thermal lens. A second TEM_{00} Gaussian beam, which is collinear with the excitation beam is incident to the sample to probe the thermal lens. The position of the probe beam (ω_{op}) is taken as the origin along the axis Z. A sample cell of length l is located at Z_1 and the detector plane is positioned at distance Z_2 from the cell. The radii of the probe beam and the excitation beam in the cell are ω_p and ω_e respectively. Shen et al. [16] have recently developed a cw laser induced thermal lens quantitative model which precisely describes the behavior of a mode-mismatched spectrometer. The steady-state signal may be expressed by using:

$$TLs = \frac{I_0 - I_\infty}{I_0}$$

$$= 1 - \left[1 - \frac{\theta}{2} tan^{-1}\left(\frac{2m(Z_1/Z_c)}{1 + 2m + (Z_1/Z_c)^2}\right)\right]^2 \quad (2)$$

Where Z_c is the confocal distance, the degree of mode mismatched m, is given by

$$m = (\omega_p/\omega_e)^2 \quad (3)$$

and θ is

$$= -\left[\frac{P_e(dn/dT)}{k\lambda_p}\right]A \quad (4)$$

where P_e is the total power of the excitation laser beam, and n is the sample refractive index, k is the thermal conductivity, λ_p is the wavelength of the probe beam and the absorbance $A = \varepsilon lc$, where ε is the molar absorption coefficient and c is the concentration of the solution.

From expression (4) we could see that the choice of the solvent for the TLs measurement looks to be one of the most important experimental parameters. Non-polar or slightly polar or slightly polar organic liquids are used to obtain a strong signal owing to their high values of dn/dT and low k values.

In this work, we developed and optimized a mismatched dual beam thermal lens spectrometer for sensitive quantitative analysis of trace amounts of vanadium species in solution. The system was tested for the detection of V in aqueous and ethanol-water [(2+3 v/v) and (4+1 v/v)] solutions of vanadium peroxide complex (HVO_4).

The effects and interactions among some experimental factors that determine the thermal lens signal are reported. Optimization of these factors was realized by using factorial study and univariate optimization methods.

Experimental

Instrumental

Optics. The thermal lens spectrometer was based on a collinear dual-beam configuration; a schematic diagram of the apparatus is shown in Fig. 2. A Coherent Innova 300 argon ion laser (514.5 nm) was used as a pump beam. The excitation beam, which was amplitude modulated by a mechanical shutter was focused onto the

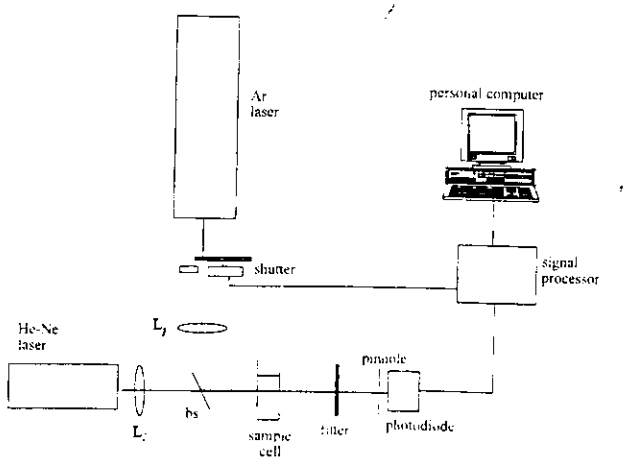

Fig. 2. Schematic representation of a dual beam thermal lens spectrometer system. L_1 and L_2 are convergent lenses and bs is a beam splitter

Table 1. Relationship between factor levels and coded values for the full two level three factor factorial study

	Coded value	
Factor	−1	+1
b/μm	20	150
Z_1/cm	14	50
Z_2/cm[a]	−7.5	5

[a] Negative or positive values indicate that the waist of the probe beam is located before or after the sample cell respectively.

sample cell with lens L_1 (200-mm focal length). A 5 mW He-Ne laser (model 05-LHR-151 Melles Griot, 632.8 nm) was used as probe beam and focused with lens L_2 (200-mm focal length). A 10 mm path quartz spectrophotometric cuvette was used as the sample cell. A 50% beam splitter was used in order to direct collinearly the excitation and the probe beam through the sample cell. In order to allow the movement of the sample cell and the excitation and probe lens along the directions of the laser beams, a special mount was used. The transmitted excitation beam was blocked after the sample with an absorption filter. The thermal lens signal was obtained by sampling the intensity at the center of the probe beam with a precision pinhole and a silicon photo diode (Melles Griot LM2). The detector-pinhole system was mounted in an XYZ translator in order to localize the laser beam center and to change the cell-detector distance. The photocurrent was amplified by a trans impedance amplifier (Melles Griot 13-AMP-003).

Data Processing

The amplified photo current was digitized using a personal computer (AT 386) with an ADC/DAC board (Lab-PC card, National Instruments). The sampling rate used was 200 samples/seconds. In order to measure the intensity variation of the probe beam (I_0-I), the DC level was subtracted from the signal by using a differential amplifier. The initial intensity of probe beam (I_0) was taken at the beginning of each shutter pulse. Both signals were acquired by the computer and then averaged using a digital multichannel averager software program.

Reagents. A stock solution of 1000 mg l^{-1} in water was prepared from ammonia meta vanadate (Aldrich Chemicals 99.9%). Lower concentration solutions were prepared by dilution of stock solution with high purity water. Analytical reagent grade nitric acid and hydrogen peroxide from BDH were used. The alignment procedures were carried out with a 50 mg l^{-1} solution of vanadium peroxide complex.

Vanadium complex preparation. The procedure for vanadium determination involves the preparation of pervanadic acid (HVO_4), which is obtained by reaction of vanadium (V) solution with hydrogen peroxide in nitric acid medium (2M) [16]. Under this condition it could be assured that all vanadium will be present as the (V) oxidation state. The absorptivity (a) obtained from the absorption spectrum of this complex at 514 nm was 0.0381 $g^{-1}cm^{-1}$.

Chemometrics

Full two-level three-factor factorial. Factorial designs [18] are powerful tools in order to measure both the effects of the factor on a response and the interaction among factors (by the effect of a factor, the change in the response in moving from the lowest to the highest level of that factor is meant). These consist of all the possible combinations of levels from the different factors.

The first step in the formulation of a factorial design is the selection of the factors affecting the signal. According to Eq. (2) for a dual-beam mode mismatched configuration, the TLs depends on the excitation laser beam power and the degree of mode mismatching m.

The thermal lens signal dependence upon power density is known to be linear and strong. Therefore, the power of the excitation beam was fixed and it was focused on the center of the sample cell in order to maintain the maximum power density.

The Z_1 distance and consequently the probe beam laser waist at the cell (ω_p) were changed, varying the position with respect to the cell of the focusing lens used to collimate the probe beam laser. The power at the detector depends on the pinhole diameter b and the detector position Z_2 [20]; hence these were selected as the two other important variables to be considered in our experimental design.

Initially, a full two-level three-factor factorial study on the thermal lens signal (TLs) was designed with the factors remaining i.e.: the size of the aperture (b), the distance from the sample to the detector (Z_2), and the distance from the sample to the waist of the probe beam (Z_1) as defined in Fig. 1. The three factors and their relationship between factor levels are given in Table 1. These combinations were performed in random order.

Results and Discussion

Factorial Study

All studies were made using a 50 mg l^{-1} vanadium peroxide complex solution. The effective width of the excitation beam, located at the sample cell center was 0.11 mm. The incident power used was 208 mW.

The experimental TLs values measured for each of the combinations of parameters in the factorial design are given in the Table 2.

The complete analysis of variance for the factorial design is summarized in Table 3. The F test shows that b, Z_1 and the interaction $b \times Z_2$ were the only ones statistically significant at 1%.

Table 2. Experimental values of TLs obtained for a 50 mg l^{-1}, vanadium peroxide solution at each of the combinations of parameters in the factorial design

	b(μm)			
	20		150	
	Z_2 (cm)		Z_2 (cm)	
Z_1(cm)	14	50	14	50
−7.5	0.30	0.161	0.147	0.170
5	0.47	0.42	0.358	0.38

All values correspond to the average of five replicates.

Table 3. Analysis of variance for TLs signal

Source of variation	Sum of squares	Degrees of freedom	Mean squares	F Ratio	Significance
Main effects					
b	0.0109	1	0.0109	15.36	0.0001
Z_1	0.0903	1	0.0903	126.69	0.0000
Z_2	0.0026	1	0.0026	3.64	0.0565
Two factor interactions					
$b \times Z_1$	0.0068	1	0.0068	9.60	0.9168
$b \times Z_2$	0.0000	1	0.0000	0.01	0.0019
$Z_1 \times Z_2$	0.0010	1	0.0010	1.36	0.2439
Total error	0.0010	7	0.0010	1.42	0.2334
External sigma[a]			0.0007		

[a] The external sigma was determined using genuine replicated runs.

Table 4. Calculated effects and standard errors for the 2^3 factorial design

Effect	Estimate error standard
Average	0.30075 ± 0.00944
Main effects	
b	-0.074 ± 0.01888
Z_1	0.212 ± 0.01888
Z_2	-0.036 ± 0.01888
Two factor interactions	
$b \times Z_1$	-0.002 ± 0.01888
$b \times Z_2$	0.0585 ± 0.01888
$Z_1 \times Z_2$	0.022 ± 0.01888

The effects calculated from factorial analysis are collected in Table 4. The distance Z_1 has a positive effect on the TLs of 0.2125. The effects of the b Z_2 can not be interpreted separately because the large interaction. The positive sign of the interaction predicts that the larger TLs will be reached to combinations of short Z_2 distance with small aperture or long Z_2 distance with large aperture.

Optimization

Probe beam waist-cell distance (Z_1). The optimization of the distance Z_1 can be carried out using an univariate method because this factor has no interactions with the others factors.

This study was carried out using $Z_2 = 11.5\,\text{cm}$, $b = 20\,\mu\text{m}$ and a $50\,\text{mg}\,\text{l}^{-1}$ vanadium peroxide complex solution. Figure 3 shows the TLs signal as a function of the distance Z_1. Positive and negative values of the Z_1 distance correspond to focus positions before and after the sample cell, respectively. From Fig. 3, the lowest TLs values are obtained for negative

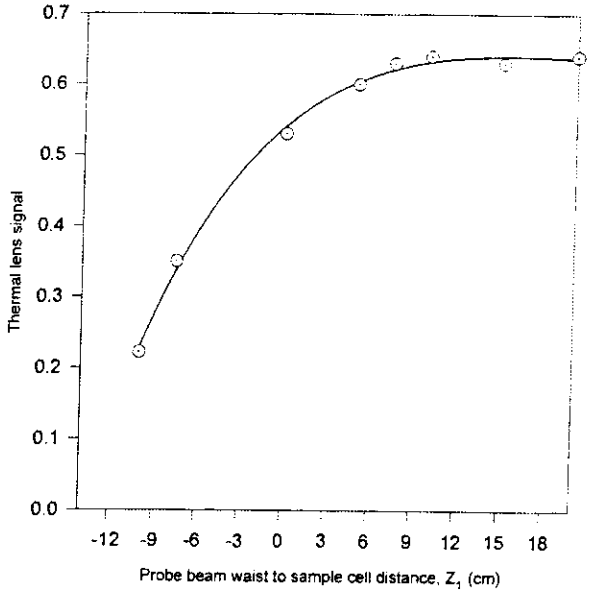

Fig. 3. Thermal lens signal Z_1 distance dependence. Laser pump power 208 mW, Z_2 distance 11.5 cm, optical aperture 20 μm and $50\,\text{mg}\,\text{l}^{-1}$ solution pervanadic acid concentration

Z_1 values. For $Z_1 > 0$ the TLs increases slightly as the Z_1 distance increases. It is observed that there is not an appreciable increase for values of Z_1 greater than the confocal distance of the probe beam (6 cm). A physical explanation of the curve could be addressed to the existence of a divergent thermal lens generated in the cell. If the probe beam waist is placed before the divergent lens simply the divergence of the beam will be increased. On the other hand, if the waist is placed after the divergent lens divergence will be decreased.

Figure 4 shows the experimental thermal lens signal and the theoretical values predicted by Eq. (2) as a function of the degree of mode mismatched m (Eq. (3). The values predicted by the model proposed by Shen et al. [16] are in good agreement with the data obtained. For m values lower than 15, the TLs increases at a very fast rate with m. For greater values, the signal increases only slightly with m.

Strong Z_1 dependence of the calibration curves linearity has been reported [6]. In order to evaluate this dependence, calibration curves were made in the 0 to $1\,\text{mg}\,\text{l}^{-1}$ vanadium complex concentration range. The linearity of the calibration curves was strongly affected by Z_1 values as is shown in Fig. 5. The wide linear calibration range and the best sensitivy were obtained for a Z_1 distance equal to 6 cm (close to Z_c).

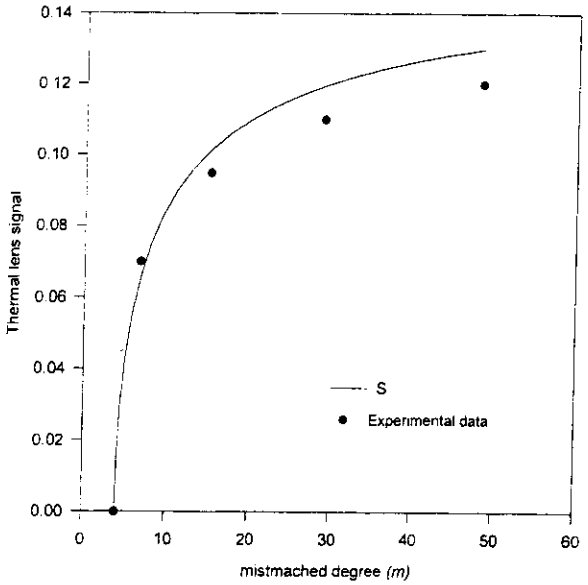

Fig. 4. Experimental thermal lens signal and theoretical values predicted by the model for mode-mismatched thermal lens spectrometry developed by Shen et al. [15] versus mode mismatched degree (m)

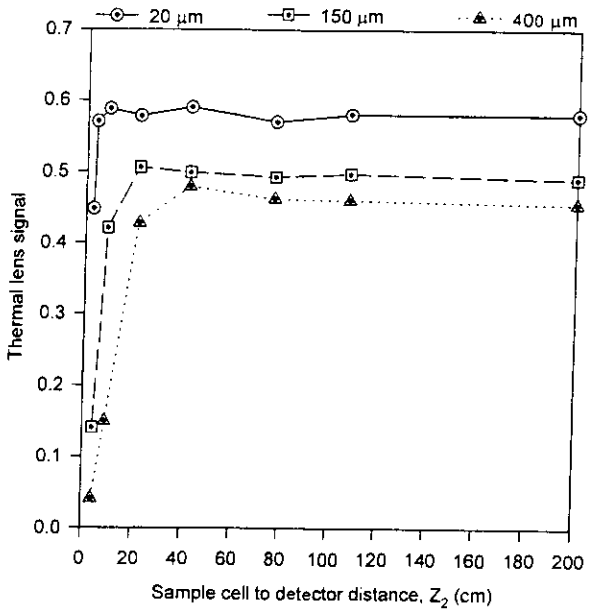

Fig. 6. Thermal lens signal Z_2 distance dependence for 20, 150 and 400 µm diameter aperture. Laser pump power 208 mW, Z_1 distance 6 cm, and 50 mg l^{-1} solution pervanadic acid concentration

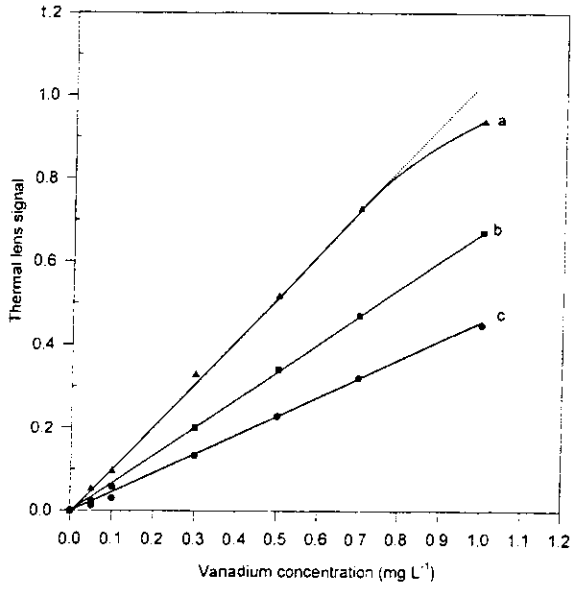

Fig. 5. Obtained calibration curves using different Z_1 values. 0 cm (a), 6 cm (b), 12 cm (c)

For this reason we selected a 6 cm Z_1 distance as the optimal value.

Cell-detector distance (Z_2) and aperture (b). As a result of the factorial study, the optimizations of the Z_2 distance and aperture b should have been realized in a multivariate form. But the lack of calibrated pinholes made that impossible to be satisfied. So the optimizations were performed using one aperture at a time. Figure 6 shows the TLs as a function of the distance from the sample cell to the detector (Z_2), obtained for three different apertures (20, 150, and 400 µm). The plotted points are the averages of three measurements. For each aperture, initially, the TLs increases linearly with the Z_2 distance up to maximum and then tends to be constant. This phenomenon is theoretically predicted by using a Fresnel diffraction theory of laser beam propagation [21]. Maximums for 20, 150 and 400 µm apertures are observed at Z_2 values 11, 23, and 40 cm respectively. It is clearly noticed that the largest TLs is always obtained for 20 µm aperture. However, the experimental work with that small aperture was very tedious due to TLS high sensivity to mechanical vibration and unstable pointing of the lasers. The maximum signal obtained with a 150 µm aperture is around 87% of the maximum signal level obtained. This aperture provides a relative good TLs and minimizes problems associated with smaller apertures. We selected a 150 µm aperture and 23.5 cm Z_2 distance as the optimal values. This results demonstrated that good sensivity could be obtained by using a relative short cell-detector distance and adequate pinhole diameter resulting in a compact instrument configuration.

Table 5. Estimated parameters of the calibration curves obtained for the vanadium complex in water and ethanol-water solutions

	Slope ± SD[a]	Intercept ± SD[a]	R^2	Detection limits (mg/l)
Water	0.424 ± 0.003	0.0193 ± 0.0008	0.999	0.0071
Ethanol-water (2+3 v/v)	0.923 ± 0.005	0.050 ± 0.001	0.999	0.0065
Ethanol-water (1+4 v/v)	1.54 ± 0.01	0.150 ± 0.002	0.999	0.0039

[a] Standard deviation.

Limit of Detection

Calibration curves for the vanadium complex in water, ethanol-water (2 + 3 v/v) and ethanol-water (4 + 1 v/v) were obtained over a concentration range of 0 to 1 mg l^{-1}, using the optimized values: aperture diameter (150 μm), cell to detector distance (23.5 cm), probe beam waist to cell distance (6 cm) and the power density of the excitation beam at the sample cell 2650 W/cm^2. Table 5 shows the statistical parameters obtained for three calibration curves and detection limits obtained. The detection limit, defined as the amount of the sample that yielded a signal three times the standard deviation of the blank [22], was estimated to be 0.0071, 0.0065 and 0.0039 mg/l in aqueous and ethanol-water (2 + 3 v/v) and (4 + 1 v/v) solutions respectively. The last solvent combination has been reported to be the best for thermal lens analytical application [6]. The absorption coefficient of the vanadium complex was evaluated in the two used solvents by using a UV-visible spectrophotometer (Perkin Elmer Lambda 3). The experimental results show that the absorption coefficient remains unchanged in both solvents. This fact means that the sensivity increase can not be attributed to changes in the absorption coefficient and must be explained by changes in the enhancement factor (E) due to the increase in dn/dT and decrease in k values in the ethanol-water mixtures.

Conclusions

Experimental design techniques have demonstrated to be a unique and useful way to establish the influence and interaction of different optical physical parameters on the TLs sensitivity. The factorial designs showed that, in the range of conditions studied, the effects of the distance from the sample to the probe beam waist (Z_1) and the interaction of the aperture with the distance from the sample to the detector ($b \times Z_2$) water the only ones statistically significant at 1% (Table 3). The strong ($b \times Z_2$) interaction suggests that selection of the aperture diameter must be realized in combination with an adequate Z_2 distance.

Thermal lens spectrometry has been shown to be a sensitive technique in the determination of V in aqueous and organic-water media. The detection limits for aqueous and ethanol-water [(2 + 3 v/v) and (4 + 1 v/v)] media were 0.007, 0.0065 and 0.0039 mg l^{-1} respectively. These values could be improved using a complex with a higher absorptivity than the one of the peroxovanadic acid. The sensitivity obtained with the thermal lens technique clearly surpasses that of ordinary spectrophotometry by many orders of magnitude [2] and is competitive with that obtained in atomic spectroscopic techniques such as graphite furnace atomic absorption and inductively coupled plasma atomic emission [23]. It should be noticed that the presence of organic solvents allows an improvement of the vanadium detection limits when is compared with those obtained in water solutions. This fact stablish a clear advantage in the analysis of oil and oil derivates products over other techniques such as ICP-AES, which, present a poor performance in these kinds of samples [25].

Acknowledgement. This work was supported by the CONICIT-Venezuela grants S1-2226 and S1-95000574 and the Consejo de Desarrollo Científico y Humanístico de la Universidad Central de Venezuela grant 03-12-3687-96.

References

[1] B. Patel, G. E. Henderson, S. Haswell, R. Grzeskowiak, *Analyst* **1990**, *115*, 1063.
[2] M. J. Taylor, J. F. Van Staden, *Analyst* **1994**, *119*, 1263.
[3] J. M. Harris, N. J. Dovichi, *Anal. Chem.* **1980**, *52*, 695A.
[4] K. Mori, T. Imasake, N. Ishibashi, *Anal. Chem.* **1982**, *54*, 2034.
[5] D. Rojas, R. Silva, J. Spear, R. Russo, *Anal. Chem.* **1991**, *63*, 1927.
[6] A. Abroskin, T. Belyaeva, A. Filichkina, E. Ivanova, M. Proscurnin, V. Savostina, Y. Barbalat, *Analyst* **1992**, *117*, 1957.
[7] R. D. Snook, R. D. Lowe, *Analyst* **1995**, *120*, 2051.
[8] D. Tran Chieu, *Appl. Spectrosc.* **1987**, *41*, 512.
[9] M. Sikovec, M. Novic, V. Hudnik, M. Franko, *J. Chromatogr. A.* **1995**, *706*, 121.
[10] J. M. Harris, in: *Analytical Application of Laser* (E. H. Piepmeier, ed.), Wiley-Interscience, New York, 1986, p. 451.
[11] H. L. Fang, R. L. Swofford, in: *Ultrasensitive Laser Spectroscopy* (D. S. Kliger, ed.), Academic Press, New York, 1983, 176.

[12] N. J. Dovichi, J. M. Harris, *Anal. Chem.* **1979**, *51*, 728.
[13] K. Nakanishi, T. Imasaka, N. Ishibashi, *Anal. Chem.* **1985**, *57*, 1219.
[14] J. Power E. D. Salin, *Anal. Chem.* **1988**, *60*, 838.
[15] T. Berthoud, N. Delorme, P. Mauchien, *Anal. Chem.* **1985**, *57* 1216.
[16] J. Shen, R. D. Lowe, R. D. Snook, *Chemical Physics* **1992**, *165*, 385.
[17] J. Basset, R. C. Denney, G. H. Jeffrey, J. Mendham (eds.), *Vogel's Textbook of Quantitative Inorganic Analysis, 4th Ed.*, Longman, Harlow, 1979.
[18] Ch. Bayne, I. Rubin, *Practical Experimental Designs and Optimization Methods for Chemists, 1st Ed.*, VHC, Weinheim, 1986, p. 69.
[19] G. E. P. Box, W. G. P. Hunter, J. S. Hunter, *Statistics for Experimenters: An Introduction to Designs, Data Analysis and Model Building, 1st Ed.*, Wiley New York, 1978. 306.
[20] A. Yariv, *Optical Electronics, 3rd Ed.*, Holt. Rinehart. Winston, New York, 1985.
[21] S. Wu, N. J. Dovichi, *J. Appl. Phys.* **1990**, *67*, 1170.
[22] J. C. Miller, J. N. Miller *Statistics for Analytical Chemistry, 1st Ed.*, Wiley, New York, 1984, 97.
[23] M. Parsons, S. Major, *Appl. Spectrosc.* **1983**, *5*, 411.
[24] S. Hill, J. Dawson, W. Price, I. Shuttler, J. Tyson. *J. A.A.S.* **1996**, *11*, 35R.
[25] P. Keliher, in: *Inductively Coupled Plasma in Analytical Atamic Spectrometry* (A. Montaser, D. Goligtly. ed.) VCH, New York, 1987, 601.

Received November 5, 1996. Revision May 19, 1997.